Bulletin of the Seismological Society of America. Vol. 64, No. 5, pp. 1419–1428. October 1974

TIME FUNCTIONS APPROPRIATE FOR DEEP EARTHQUAKES

BY L. J. BURDICK AND D. V. HELMBERGER

ABSTRACT

The seismic signatures of isolated body phases from many deep-focus earthquakes were analyzed in the time domain. Most shocks were found to be multiple events when examined in detail. The time history derived from *P* waves for single events predict synthetic *S*-wave shapes that match the observations, indicating compatibility with shear dislocation theory. Several other features of source functions in the time domain have been brought to light.

INTRODUCTION

Recent studies on *P* and *S* spectra such as Hanks and Wyss (1972), Wyss and Molnar (1974), and Molnar *et al.* (1974) indicate that on the average the spectral corner frequency (Brune, 1970) of *P* waves is significantly higher than that of *S* waves. Savage (1972) demonstrated that these results are incompatible with shear dislocation theory. Because the Haskell (1964) dislocation model has the advantage of being both logically straightforward and mathematically simple, it seems worthwhile to focus sharply on this discrepancy to be certain that it reflects a breakdown in the model. Accordingly, in this study, we have attempted to isolate in the time domain any differences between *P* and *S* sources beyond those predicted by shear dislocation theory to make sure such differences exist and, if they do, to understand why.

The spectral corner-frequency studies have made use of three different types of observations; local (Molnar *et al.*, 1974), shallow teleseismic (Hanks and Wyss, 1972), and deep teleseismic (Molnar and Wyss, 1972). The local high-frequency events were recorded near the epicenter on horizontal instruments. This recording geometry provides a natural prejudice against *P* waves. In the case of shallow events, the spectra were severely contaminated by free-surface effects (Helmberger, 1974) which casts some doubt upon the results. The results from the deep events were the most significant and the ones which we elected to re-examine in this study. Although, in contrast to the previous study of deep events, we chose to compare the *P* and *S* sources in the time domain.

Transforming a time series into the frequency domain for analysis does provide many computational advantages, but it also masks information about the sequence and duration of transient pulses. However, an analysis in the time domain preserves this information. Therefore, a comparison of the *P* and *S* wave forms should help to isolate on the record precisely when and how the *S* pulse departs from the shape predicted by shear dislocation theory.

We have used a two-stage procedure in studying the *P* and *S* waves. First, we determined the far-field time history from digitized *P* waves by deconvolution. Next, we generated synthetic *S* waves assuming the same time history for comparison with observations. We chose this course over the more obvious one of deconvolving to obtain the *S* source and comparing with the *P* source for these reasons. Our technique permits direct comparison of calculated results with unprocessed data, and it permits us to circumvent the large uncertainties associated with deconvolution. That is, when a bandpass filter like a seismic instrument is deconvolved from a signal such as the *P*-wave form, the uncertain data well off the filter peak are heavily emphasized. However, when the

result is reconvolved with the filter in producing the synthetic S, the uncertain data is again de-emphasized.

OBSERVATIONS

The data-set consists of observations of three deep events from three source regions. The events were selected on the basis of their size, the character of their wave forms and their location relative to observing stations. All three earthquakes have a body-wave

TABLE 1

SELECTED EARTHQUAKES

Location	Latitude (S)	Longitude	Date	Time	Depth (km)	Magnitude
Argentina	27.4	63.3	1/17/67	1: 7:54.3	590	5.5
Fiji	21.1	179.2	3/17/66	15:50:33.1	639	6.2
W. Brazil	9.1	71.4	3/11/65	1:39: 3.1	593	6.2

TABLE 2

LOCATION OF THE WWSSN STATIONS RELATIVE TO EVENTS

Event	Observing Stations	Distance (deg)	Azimuth (deg)
Argentina	BLA	66.3	345
	QXF	66.3	337
	JCT	67.3	326
	SCP	69.2	348
	AAM	71.9	344
	ALQ	74.2	324
	BEC	76.4	358
Fiji	BAG	69.8	296
	ANP	73.7	305
	HKC	78.0	300
W. Brazil	LUB	51.3	327.2
	ALQ	54.9	324.8
	TUC	55.8	319.5
	RCD	60.3	334.1

magnitude, roughly of 6. At this size they are large enough to provide strong teleseismic signals, but small enough to simplify the predictions of the shear dislocation theory as will be explained later. The wave forms of both the P and the S were required to be well defined and impulsive in character, leaving no doubt as to the onset and termination of the phase. Finally, the events had to occur at an epicentral distance of 50° to 80° from a small array of WWSSN stations. Acting together, these three conditions served to severely limit the available data-set. An extensive search of the WWSSN records was required to produce the three events used in this study. The pertinent source information is given in Table 1 and the station data, in Table 2.

The S observations were rotated into SH and SV components and the better resolved of the two was selected for the study. SH is ordinarily preferable because it contains no converted phases. However, inasmuch as its radiation pattern is orthogonal to P,

whenever the P wave is strong and clear, the S is primarily SV. Consequently, SV waves were used for the Western Brazil and Fiji events and SH for only the Argentina event.

Calculation of Synthetics

Computation of a synthetic seismogram involves modeling the effects of rupture propagation, attenuation, instrument response and earth structure on some specified source-time function. In shear dislocation theory, the effects of rupture propagation can be modeled by convolving a boxcar function of duration

$$\Delta t = \frac{L}{2}\left(\frac{1}{V_r} - \frac{\cos\delta}{(\alpha, \beta)}\right)$$

with the source-time history. L is the fault length, V_r the rupture velocity, δ the angle between the rupture direction and the ray direction and (α, β) is either the P or S velocity, depending on the respective wave type. Mikumo (1971) demonstrated empirically that the azimuthal variation of the rupture effect disappears for earthquakes of magnitude 6 or less. If the azimuthal dependence vanishes, the wave-type dependence also vanishes which implies that for the three events used in this study the P-source function and rupture effects should be identical with the S. This result of shear dislocation theory is the one which we tested by computing synthetic S waves from P source functions.

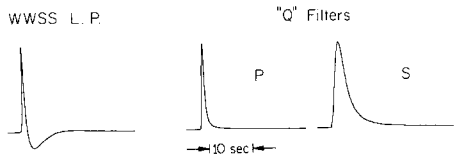

FIG. 1. Delta-function response of the WWSS long-period instrument and attenuation filters.

(From this point forward, the term "source function" includes the rupture effect.) Any significant difference between the observed and synthetic S wave should indicate either a difference in P and S sources beyond those predicted by theory or earth structure which has not been accounted for.

Past work has shown that the Q operator for the Earth is nearly independent of frequency (Attewell and Ramona, 1966). The Fourier amplitude at some point along the ray path defined by x may be written as a function of frequency ω and wave velocity c as

$$A(\omega) = \exp\left(-\omega \int \frac{dx}{2cQ(x)}\right).$$

The expression can be further simplified by replacing $Q(x)$ with a constant average Q and obtaining

$$A(\omega) = \exp(-\omega T/2Q)$$

where T is the travel time (Carpenter, 1967). The quantity T/Q is a near-constant (Helmberger, 1973a) and was assumed in this study to be 0.55 for P and 2.2 for S (Anderson *et al.*, 1965). The time-domain pulses of the Q filters are shown on the right of Figure 1.

The pulse next to the filters is the delta function response of the WWSSN long-period Benioff. The steady-state response of the instrument and Q filter pulses have been tested by convolving them with infinite sinusoids of various frequencies. The agreement with the expected Fourier amplitudes is most satisfactory.

The earth structure correction for deep earthquakes such as these can be handled almost as simply as the rupture effect. The free-surface effects are negligible; the mantle structure effects become negligible if the observed rays bottom in the smooth lower mantle (Helmberger, 1973b), which leaves only the structure near the receiver. It would be unreasonably tedious to attempt to model the structure near every station which was used, but an approximation to the amplitudes and arrival times of all the important near-source reflected phases, except one, can be computed using the Haskell unilayered crust model and plane-wave theory. The theory breaks down for the one case of *SV* coupled *PL* because the ray parameter for this phase is relatively large. The *PL* phase is extremely difficult to model using even more sophisticated techniques because it is highly sensitive to variations in crustal structure. Consequently, no attempt has been

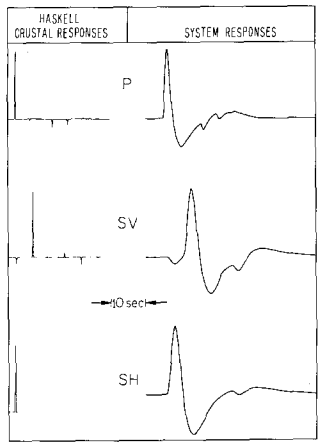

FIG. 2. Delta-function response for the crust and earth-instrument system.

made to synthesize the *PL* phase. Fortunately, only one of the three earthquakes contained a possible *PL* arrival and it occurred late enough in the wave to be easily discriminated from source information. The delta function responses of the crust for *P*, *SH* and *SV* incident plane waves are shown on the *left* of Figure 2. The system responses derived by performing a double convolution involving the instrument, *Q* operator, and crustal responses are displayed on the *right*.

DETERMINATION OF THE TIME FUNCTION

The most obvious way to find the source function given the *P* observation and system response is to deconvolve. Accordingly, for each of the three earthquakes, the *P*-system response was deconvolved from several high-quality *P* observations. The resulting time functions were cross correlated and averaged at the time of peak correlation. The observing stations were chosen in tight patterns, so that if there were an azimuthally varying difference in the *P* and *S* sources, it would be emphasized rather than smoothed by the averaging. The results are shown in Figure 3. The dotted standard deviation line gives some indication of the variation of the deconvolved pulses. The *middle column* gives the integral of the time function which should correspond to the average motion on the fault somewhat smoothed by rupture effects. The *right-hand column* shows the Fourier transform of the source function in a frequency band appropriate for the sampling rate and signal length. The three sources show significant variation in structure and,

as demonstrated most clearly in the *middle column*, they show a feature somewhat similar to an overshoot.

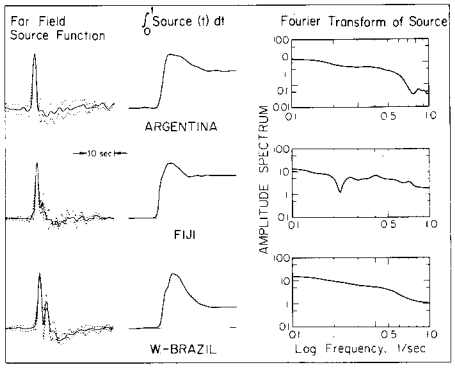

FIG. 3. Source functions deconvolved from averaged *P* waves are displayed on the *left*. The dislocation history across the fault produced by integration are displayed in the *middle column*. The corresponding amplitude spectra are given on the *right*.

RESULTS

The deconvolution and averaging technique was tested by convolving the source functions with the *P*-system responses to reproduce the *P*-wave forms. The results on the *left* of Figures 4 and 5 indicate that we have produced a satisfactory representation of the *P* source. The synthetic *S* waves on the right of the figures were computed by convolving the *P* source with the *S*-system function. For the Argentina and Fiji events, there is no significant difference between the observed and synthetic *S* waves. The

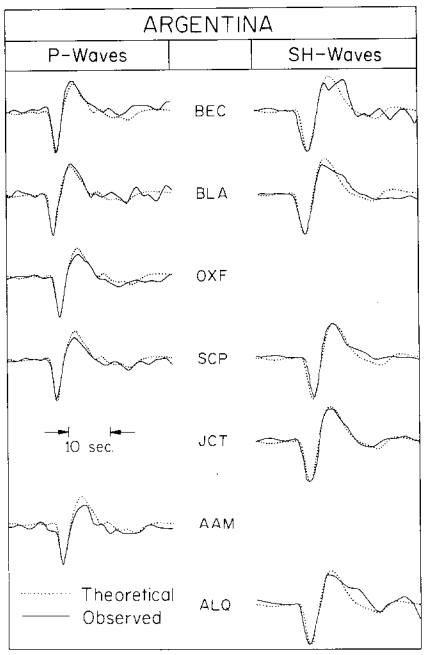

FIG. 4. A comparison of the synthetic *P*- and *S*-wave forms with the observed signals.

synthetic of the Western Brazil *S* does diverge from the observations, but this may be linked to an *SV* coupled *PL* arrival. The relatively high-frequency pulse arrives roughly 10 sec after onset. This is too large a time span for the fault to be still radiating but does correspond to *PL* arrival time. Also note the wide variation in form over the compact station array. This is again characteristic of the *PL* phase.

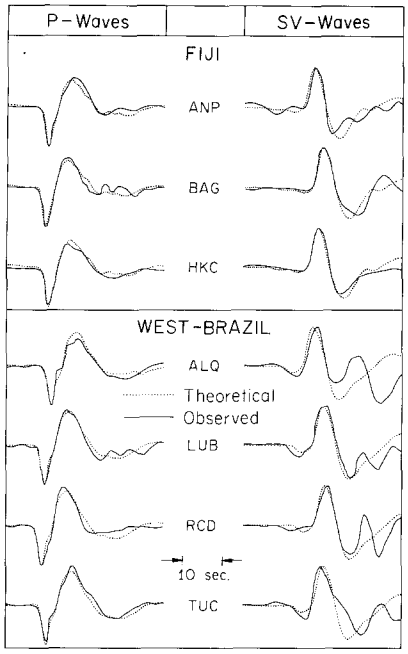

FIG. 5. A comparison of the synthetic *P*- and *S*-wave forms with the observed signals.

DISCUSSION

The close agreement between the observed and synthetic *S* waves for the Argentine and Fiji events indicates that, for magnitude 6 earthquakes at teleseismic distances, the *P*- and *S*-source functions are nearly identical as predicted by the Haskell dislocation model. Contrastingly, the Wyss and Molnar (1972) study indicated a difference in the spectral corner of *P* and *S* for highly similar data. Providing that both analyses are correct, this indicates that the corner-frequency difference is only weakly constrained by the original time-domain data and raises the possibility of the difference being an artifact of the data processing. The occurrence of a strong *PL* phase in the Western Brazil *S* wave demonstrates that even for deep earthquakes at ranges greater than 50°, earth structure can distort the wave shape and the Fourier spectrum. Any future studies of this type in either the frequency or time domain should be coupled with a careful examination of the seismograms to screen out data contaminated by not only *PL*, but *PcP* and *ScS* as well.

As was noted, an important advantage of the time domain is that information about sequence and duration is preserved. That is, the time function of the Western Brazil earthquake in Figure 3 clearly indicates that there were two high-frequency events. However, this information is not apparent from the amplitude spectrum. What is apparent is that the two peaks enhance the short periods relative to the long. In a corner-frequency study this would have the surprising effect of decreasing the estimated source

dimension. A time-domain study would permit the events to be analyzed separately yielding two sets of source parameters. The difficulties associated with double sources may warrant some attention because, of five deep earthquakes analyzed in this and a subsequent study, three have been shown to contain more than one event.

One other feature of the source function that merits some attention is the overshoot-like phenomenon. It does not appear to be a spurious effect of the data processing for two reasons. First, the feature does not appear when the same procedure is used on shallow earthquakes; and second, the phenomenon is directly observable in the phase *pP*. It is not difficult to see that, if the time functions shown in Figure 3 were strongly filtered

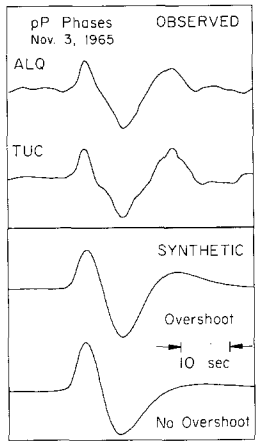

FIG. 6. A comparison of the synthetic *pP* phases computed with and without overshoot (artificially removed) with the observed *pP* signals.

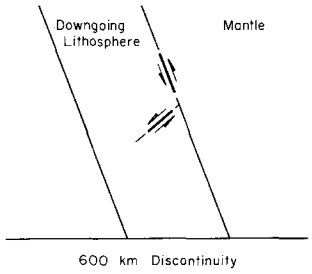

FIG. 7. A hypothetical set of planes along which a high-frequency shock inside the plate might couple to a low-frequency shock on the plate boundary.

by propagating twice through the low Q layers at the Earth's surface, the main peak would be more strongly affected than the backswing. The pulse would have, roughly, equal area up and down swings. The instrument response to such a pulse would have three swings instead of two. The *bottom two traces* of Figure 6 show synthetic *pP* arrivals from the Western Brazil source. The overshoot was artifically removed in the *lower trace*. The *top two traces* show observed *pP* phases.

There are at least three possible explanations for the backswing. First, it may represent actual return motion on the fault. Burridge (1969) obtained a theoretical result for motion on a frictionless fault which did overshoot and return. He reasoned that in real earthquakes friction would prevent this from happening. Perhaps for deep events, there is

melting on the fault which keeps friction from playing an important role. Second, the backswing may reflect motion on the surface between the down-going plate and the mantle. Fault plane studies have indicated that most deep shocks occur inside the plate. The mantle plate surface appears to allow relatively smooth motion; but this surface is still a plane of weakness which may interact with a rupture in the plate. A coupled set of motions like those shown in Figure 7 would explain the sense of motion of the initial swing and the backswing for all three events. Note that the long slow backswing is consistent with the mantle-plate coupling being weak in nature. The third possible explanation is that the backswing is a volume source effect (Archambeau, 1968) and should not be interpreted at all as motion on a fault surface.

Conclusions

As predicted by the Haskell shear dislocation theory, there are no strongly resolved differences between P and S sources on long-period seismograms for deep events of magnitude 6. This study has also shown that seismic sources should in many, if not most, instances be considered as sums of simpler events which may even have different fault planes.

Acknowledgments

The authors thank Ralph Wiggins for his advice and for the use of his deconvolution program. This research was supported by the Advanced Research Projects Agency at the Department of Defense and was monitored by the Air Force Office of Scientific Research under Contracts F44620-72-C-0078 and F44620-72-C-0083.

References

Anderson, D. L., A. Ben-Menahem, and C. B. Archambeau (1965). Attenuation of seismic energy in the upper mantle, *J. Geophys. Res.* **70,** 1441–1448.

Archambeau, C. B. (1968). General theory of elastodynamic source fields, *Rev. Geophys.* **6,** 241.

Attewell, P. B. and Y. V. Ramana, (1966). Wave attenuation and internal friction as functions of frequency in rocks, *Geophysics* **31**, 1049–1056.

Brune, J. N. (1970). Tectonic stress and the spectra of seismic shear waves from earthquakes, *J. Geophys. Res.* **75,** 4997–5009.

Burridge, R. (1969). The numerical solution of certain integral equations with nonintegrable kernels arising in the theory of crack propagation and elastic wave diffraction. *Phil. Trans. Roy. Soc. (London), Ser. A.* **265,** 353–381.

Carpenter, E. W. (1967). Teleseismic signals calculated for underground, underwater, and atmospheric explosions, *Geophys.* **32,** 17–32.

Hanks, T. C. and M. Wyss (1972). The use of body-wave spectra in the determination of seismic parameters, *Bull. Seism. Soc. Am.* **62,** 561–589.

Haskell, N. A. (1964). Total energy and energy spectral density of elastic wave radiation from propagating faults, *Bull. Seism. Soc. Am.* **54,** 1811–1831.

Helmberger, D. V. (1973a). On the structure of the low-velocity zone, *Geophys. J.* **33,** (in press).

Helmberger, D. V. (1973b). Numerical seismograms of long-period body waves from seventeen to forty degrees, *Bull. Seism. Soc. Am.* **63,** 633–646.

Helmberger, D. V. (1974). Generalized ray theory for shear dislocations, *Bull. Seism. Soc. Am.* **64,** 45–64.

Mikumo, T. (1971). Source process of deep and intermediate earthquakes as inferred from long-period P and S wave forms, deep-focus and intermediate depth earthquakes around Japan, *J. Phys. Earth.* **19,** 303–319.

Molnar, P., B. E. Tucker, and J. N. Brune (1974). Corner frequencies of P and S waves and models of earthquake sources, *Bull. Seism. Soc. Am.* **63,** 2091–2104.

Savage, J. C. (1972). Relation of corner frequency to fault dimension, *J. Geophys. Res.* **77,** 3788.

Wyss, M. and T. C. Hanks (1972). The source parameters of the San Fernando earthquake inferred from teleseismic body waves, *Bull. Seism. Soc. Am.* **62**, 591.

Wyss, M. and P. Molnar (1974). Source parameters of intermediate and deep-focus earthquakes in the Tonga Arc, *Phys. Earth Plan. Int.* (in press).

Division of Geological and Planetary Sciences
California Institute of Technology
Pasadena, California 91109.
Contribution No. 2453.

Manuscript received February 11, 1974.